

# Development of Dictionary-Based Phasor Estimator Suitable for P-Class Phasor Measurement Unit

Shaik Affijulla<sup>ID</sup>, Member, IEEE, and Praveen Tripathy, Member, IEEE

**Abstract**—The paper proposes a simple phasor estimator by utilizing the dictionary-based sparse representation of signals for control and protection applications in power system. It is also observed that the proposed method is found to be suitable for extracting the fundamental component of the signal required for protective relays with few number of samples. The simulations have been carried out to test the performance of proposed phasor estimator as per the requirements provided in IEEE C37.118.1a-2014 standard and also on a modified two-area power system. To further validate the effectiveness of proposed algorithm, it has also been tested on an analog radial power system simulator with fault in the laboratory experimental setup. The measured voltage and current signals are fed to the developed prototype of phasor measurement unit (PMU) with the proposed algorithm running for phasor estimation of signals in the power system. The real-time hardware and IEEE standard test results reveal that the proposed phasor estimation algorithm is able to estimate the phasor accurately in the presence of harmonics, decaying dc components, amplitude, and phase modulation, which are typically involved during disturbances. Furthermore, the proposed algorithm is able to estimate the phasor of a signal accurately with few measured samples, thus an analog-to-digital converter with lower sampling rate is suitable for developing a prototype of low cost P-class PMU for several applications in smart grids.

**Index Terms**—Dictionary concept, dynamic phasor estimation (DPE), phasor measurement units (PMUs), protective relay, smart grids.

## I. INTRODUCTION

MODERN power systems have seen the deployment of wide-area measurement system (WAMS) in monitoring, control, and protection of complex electric networks. To improve the effectiveness of WAMS in monitoring and control of power system, it requires to provide the accurate and reliable measurement techniques for estimation of phasors corresponding to bus voltages and line currents during abnormal or transient conditions in smart power grids. The injection of renewable power into the smart grid is witnessing the challenges in relay coordination, false tripping of circuit breakers, and reliability degradation during disturbances [1]. To address some of the above issues, significant work is done toward the development of special protection schemes

Manuscript received December 20, 2017; revised March 09, 2018; accepted March 12, 2018. Date of publication April 23, 2018; date of current version October 9, 2018. The Associate Editor coordinating the review process was Dr. Chao Tan. (*Corresponding author: Shaik Affijulla*)

S. Affijulla is with the Department of Electrical Engineering, National Institute of Technology Meghalaya, Shillong 793003, India (e-mail: shaik.affijulla@nitm.ac.in).

P. Tripathy is with the Department of Electronics and Electrical Engineering, IIT Guwahati, North Guwahati 781039, India (e-mail: ptri@iitg.ernet.in).

Digital Object Identifier 10.1109/TIM.2018.2824545

for existing network [2], [3]. Most of the algorithms for the special protection schemes are based on phasor estimated by the phasor measurement unit (PMU).

PMU, which utilizes interrange instrumentation (IRIG-B) signal from global positioning system (GPS) for estimating phasor, frequency, and change of frequency, is a key element of WAMS to monitor the electrical parameters of a large power system. The accuracy required by the PMU in estimated phasor during steady state and dynamic state is described in the standard IEEE C37.118.1a-2014. The presence of nonlinear loads, sudden variation of large loads, faults, control, and protective actions, etc., corrupt the signal with the injection of dc component, harmonics, and high frequency transients. The accurate estimation of phasor corresponding to the fundamental component for the corrupted signal is important for control and protection applications. Significant work has been done toward modeling the signal during dynamic or transient conditions, but most of them are based on higher order model [4]–[19] which may not be suitable for existing philosophy of control and protection.

Discrete Fourier transform implemented using fast Fourier transform (FFT) is one of the simple and popular algorithm to estimate the phasor from given measurements. The estimated phasor by FFT-based algorithm requires large number of samples to improve its accuracy, and hence, not suitable during dynamics or transients in the power system. For control or protection applications, it is important to estimate the phasor accurately during disturbances as discussed in the literature [7], [12], [17], [18]. Jinfeng Ren [19] suggested the use of wavelet for phasor estimation, but the kernel of mother wavelet utilized is far different from the fundamental signal of interest. Recently, the concept of utilizing higher order model to parameterize various dynamics associated with the signal has been reported in [4], [5], [7], and [13]. The present day protective relays fail to utilize these complex models, may be in the future with more advancement in relay technology, these complex model-based methods may be suitable for power system protection applications.

Similarly, in [6] and [14]–[16], second-order Taylor series is introduced to model the oscillatory behavior of signal to estimate the phasor along with the least square projection of the observation sample on the signal space. The best moving average coefficients of an autoregressive moving average model are effectively utilized to estimate the phasor of a signal in Shank's method [11]. Most of contributions available in the literature for phasor estimation during transient or dynamic conditions

utilize higher order model of the signal. But protective relays in power system require phasor related to the fundamental component of the signal during disturbance for their decision. Recently, the authors have developed few algorithms toward extracting fundamental component of the signal based on Hilbert transform [20] and convolution [21] under dynamic conditions, which tries to determine the accurate estimation of the phasor corresponding to the fundamental component of a signal.

The motivation of this paper is to develop a low-cost PMU with phasor estimation algorithm, capable to estimate the phasor corresponding to the fundamental component during dynamic or transient conditions with few number of samples per cycle and is suitable for control and protection in the smart power systems. The proposed algorithm can effectively estimate the phasor during transients by using a low-sampling-rate analog-to-digital converter (ADC) (i.e., utilizing few samples per cycle) which significantly reduces the cost in developing a prototype of P-class PMU.

The remaining paper is organized as follows: Section II describes the formulation of phasor estimation algorithm to compute the phasor of a signal under transient conditions. Section III presents the simulation study of proposed algorithm performance with other methods according to the IEEE C37.118.1a-2014 standard. Sections IV and V explores the efficacy of proposed algorithm on modified two-area test power system and by real-time implementation of experiment on radial network setup with developed PMU prototype and Section VI concludes the presented work.

## II. PROPOSED PHASOR ESTIMATION APPROACH

The proposed phasor estimator tries to estimate the phasor of the signal (1) which is generally corrupted with the presence of noise, harmonics, and decaying dc components as shown in the following equation:

$$r(t) = R_m \sin(2\pi f_{ot} t + \theta) + \Upsilon e^{-t/\tau} + \mathcal{N}(0, \sigma^2) \dots \\ + \sum_{k=2}^{10} R_k \sin(2\pi k f_{ot} t + \theta_k) \quad (1)$$

where the variables of (1) are described in Table I

The proposed phasor estimation process is broadly classified in two stages, i.e., "Coarse and Fine stages." To get a rough estimate of the phase angle of a signal, the samples of signal are first projected on the components of a primary dictionary matrix ( $\mathbf{P}$ ) and to have fine adjustment on the estimated phase angle, a secondary dictionary matrix ( $\mathbf{S}$ ) is utilized. The details of proposed method are provided in Section II-A.

### A. Sampling of the Signal

It is a normal practice to avoid antialiasing filter to overcome the delay associated with the filter for a P-class PMU. Moreover, as the signal of interest is sinusoidal and very close to the nominal frequency (i.e., typically with a deviation of  $\pm 3\%$ ), and the reconstruction of the complete signal is not involved in the proposed estimation algorithm, the sampling can be done at subNyquist rate.

In this paper, first the data corresponding to the measurement, i.e.,  $\{R[n]\}_{n=1}^N$ , is obtained by sampling the signal (1) at the rate of  $N$  samples per cycle. The choice of  $N$  determines the dimension of dictionary matrices  $P$  and  $S$ , which are constructed from the pure sinusoidal signal with nominal frequency. With the proposed algorithm, it is possible to significantly reduce the sampling rate and still have a good estimate of the phasor. The developed prototype of the PMU uses 10 samples per cycle for phasor estimation and consequently reduces the overall cost of developed PMU to estimate the phasor of a signal. The details of "Coarse and Fine estimation stages" are provided in Section II-B.

### B. Coarse Estimation Stage

Dictionary matrix  $\mathbf{P}$ , defined as primary dictionary matrix has been utilized to process the sampled vector  $\mathbf{R}$  corresponding to the data samples  $\{\mathbf{R}[n]\}_{n=1}^N$  to get a coarse estimate of phase angle of the signal.

The construction of primary dictionary matrix  $\mathbf{P}$  is based on the samples taken from a sinusoidal signal, i.e.,  $\sin(\omega t + \vartheta)$  with nominal frequency of 50 Hz is given as

$$\mathbf{P} = \begin{bmatrix} \mathbf{P}_{11} & \mathbf{P}_{12} & \cdots & \mathbf{P}_{1u} & \cdots & \mathbf{P}_{1M} \\ \mathbf{P}_{21} & \mathbf{P}_{22} & \cdots & \mathbf{P}_{2u} & \cdots & \mathbf{P}_{2M} \\ \vdots & \vdots & \cdots & \vdots & \cdots & \vdots \\ \mathbf{P}_{i1} & \mathbf{P}_{i2} & \cdots & \mathbf{P}_{iu} & \cdots & \mathbf{P}_{iM} \\ \vdots & \vdots & \cdots & \vdots & \cdots & \vdots \\ \mathbf{P}_{N1} & \mathbf{P}_{N2} & \cdots & \mathbf{P}_{Nu} & \cdots & \mathbf{P}_{NM} \end{bmatrix}. \quad (2)$$

The element value of  $\mathbf{P}$ , is defined as

$$P_{iu} = \sin(\omega t_i + \vartheta_u) \quad (3)$$

where

- $i$  varies from 1 to  $N$  and  $u$  varies from 1 to  $M$
- $\omega$  is  $2\pi f$  and  $f$  is fundamental frequency in Hz
- $t$  is a vector consisting of  $N$  samples for 20 ms with step size of 2 ms
- $\vartheta$  is a vector consisting of  $M$  samples varying from 0 to  $360^\circ$  with step size of  $\mu$ .

The inner product of the sampled vector  $\mathbf{R}$  with that of primary dictionary matrix, provides the closeness of  $\mathbf{R}$  in  $L_2$ -norm to the column of primary dictionary matrix

$$\mathbf{Q} = \mathbf{P}^T \mathbf{R}. \quad (4)$$

Thus, the index corresponding to the maximum value of vector  $\mathbf{Q}$  or the estimated coarse phase angle is the phase angle of the corresponding column of the primary dictionary matrix which results in the maximum value of inner product. Empirically, the coarse stage estimated phase angle  $\theta_{\text{cor}}$  of a signal (1) from primary transformed sequence  $Q$  can be mathematically expressed as

$$\theta_{\text{cor}} = (\lambda_Q - 1)\mu \quad (5)$$

where  $\lambda_Q$  is the location of maximum value in primary transformed sequence  $Q$  and  $\mu$  is the step size, i.e.,  $3.6^\circ$  is considered in this paper. Where  $\theta_{\text{cor}}$  is the coarse estimation of

phase angle of the fundamental component of the signal  $r(t)$ . As  $\lambda_Q$  corresponds to the index where the maximum value of  $\mathbf{Q}$  is observed, which implies that the data vector  $\mathbf{R}$  is close in  $L_2$ -norm to column vector corresponding to  $\lambda_Q$  column index of  $\mathbf{P}$  matrix. Thus, the  $\theta_{\text{cor}}$  is given in (5).

Similarly, the process is repeated over the secondary dictionary matrix to get fine adjustment to the estimated phasor with reduced complexity. The fine estimation stage is discussed in Section II-C.

### C. Fine Estimation Stage

It is observed that the estimated phase angle  $\theta_{\text{cor}}$  of (1) in coarse estimation stage consists an inherent phase error of " $\pm (\mu/2)$ " which is typically significant in terms of total vector error (TVE) according to the IEEE Synchrophasor standard [27]. The following methodology is introduced to fine tune or correct the estimated phase angle  $\theta_{\text{cor}}$ .

Let  $\mathbf{S}$  be the secondary dictionary matrix and constructed as

$$\mathbf{S} = [\mathbf{S}_{P^1} \quad \mathbf{S}_{P^2} \quad \cdots \quad \mathbf{S}_{P^r} \quad \cdots \quad \mathbf{S}_{P^M}]. \quad (6)$$

Let the inner matrices of  $\mathbf{S}$ , i.e.,  $\mathbf{S}_{P^r}$ , can be constructed as

$$\mathbf{S}_{P^r} = \begin{bmatrix} \mathbf{P}_{11}^r & \mathbf{P}_{12}^r & \cdots & \mathbf{P}_{1u}^r & \cdots & \mathbf{P}_{1M}^r \\ \mathbf{P}_{21}^r & \mathbf{P}_{22}^r & \cdots & \mathbf{P}_{2u}^r & \cdots & \mathbf{P}_{2M}^r \\ \vdots & \vdots & \cdots & \vdots & \cdots & \vdots \\ \mathbf{P}_{i1}^r & \mathbf{P}_{i2}^r & \cdots & \mathbf{P}_{iu}^r & \cdots & \mathbf{P}_{iM}^r \\ \vdots & \vdots & \cdots & \vdots & \cdots & \vdots \\ \mathbf{P}_{N1}^r & \mathbf{P}_{N2}^r & \cdots & \mathbf{P}_{Nu}^r & \cdots & \mathbf{P}_{NM}^r \end{bmatrix}. \quad (7)$$

The element value of  $\mathbf{S}_{P^r}$ , is defined as

$$\mathbf{P}_{iu}^r = \sin(\omega t_i + \vartheta_u^r) \quad (8)$$

where

$r$  varies from 1 to  $M$ ,  $i$  varies from 1 to  $N$ , and  $u$  varies from 1 to  $M$ ;

$\vartheta^r$  is a vector consisting of  $M$  samples varying from  $\alpha_r$  to  $(\alpha_r + \mu)$  with step size of  $\mu$ ;

$\alpha_r$  is a vector consisting of  $M$  samples varying from  $\mu^\circ$  to  $360^\circ$  with step size of  $\mu$ .

By inner product operation on the secondary dictionary matrix and sampled vector  $\mathbf{R}$  of (1), we will have the secondary transformed sequence  $\mathbf{Q}_{\text{sr}}$  as

$$\mathbf{Q}_{\text{sr}} = [\mathbf{S}_{P^r}]^T \mathbf{R} \quad (9)$$

where " $r = \lambda_Q$ "

Empirically, the corrective or fine stage estimated phase angle  $\theta_{\text{sr}}$  of a signal (1) from the secondary transformed sequence  $\mathbf{Q}_{\text{sr}}$  can be mathematically expressed as

$$\theta_{\text{sr}} = \xi(\lambda_{\text{sr}} - 1)\mu \quad (10)$$

where  $\lambda_{\text{sr}}$  is the location of maximum value in secondary transformed sequence  $\mathbf{Q}_{\text{sr}}$  and  $\xi$  is the corrective constant, which is computed as ratio of  $\mu$  and  $360^\circ$ , i.e.,  $\xi = 0.01$  is considered in this paper.

In the estimation of fundamental phase of (1) from  $\theta_{\text{cor}}$  and  $\theta_{\text{sr}}$ , the estimated phase angles are expressed as

$$\theta(t) = \begin{cases} \theta_{\text{cor}} - \theta_{\text{sr}}, & \text{if } (\mu/2) > \theta_{\text{sr}} \\ \theta_{\text{cor}} + \theta_{\text{sr}}, & \text{if } (\mu/2) \leq \theta_{\text{sr}} \end{cases} \quad (11)$$

### D. Estimation of Fundamental Component Magnitude

The fundamental component magnitude of the signal (1) is estimated by using least square approach and mathematically computed as

$$\mathbf{R}_m(t) = [[\mathbf{P}_*^r]^T [\mathbf{P}_*^r]]^{-1} [\mathbf{P}_*^r]^T \mathbf{R} \quad (12)$$

where  $[\mathbf{P}_*^r]$  is a column vector of inner matrix,  $S_{P^r}$  corresponding to the location  $\lambda_{\text{sr}}$ , i.e.,  $[\mathbf{P}_*^r]$  is the closest vector to the sample vector ( $\mathbf{R}$ ) scaled by signal magnitude ( $R_m(t)$ ) in  $L_2$ -norm.

Thus, the inner product of sampled vector  $\mathbf{R}$  of the signal (1) with precalculated dictionary matrices, i.e.,  $\mathbf{P}$  and  $\mathbf{S}$ , which are constant and stored in buffer memory, provides the robust estimation of phase (11) and magnitude (12) of the fundamental component of a given signal.

Therefore, the above-mentioned deduced expressions (11) and (12) turn the phasor estimation process to be more simple, fast, and efficient.

### E. Estimation of Frequency and Its Rate of Change

Using Taylor series approximation, the phase angle  $\theta_{(k\Delta t)}$  of the estimated phasor is related to the frequency and changes of frequency as per the following equation [30]:

$$\theta_{(k\Delta t)} = v_0 + v_1 \Delta t + v_2 \Delta t^2 + \epsilon \quad (13)$$

where  $k = [0, 1, \dots, K-1]$  is the index of the phasor,  $\Delta t$  is the time interval between the estimated phasors,  $v_0 = \theta_0$  is the initial phase angle,  $v_1 = 2\pi \Delta f$ , where  $\Delta f$  is the frequency deviation from nominal value and  $v_2 = \pi f'$ , where  $f'$  is the rate of change of frequency,  $\epsilon$  is the error in the estimated phase angle.

Typically four or more (i.e.,  $K \geq 4$ ) phase angles of the estimated phasors are utilized to estimate frequency and rate of change of frequency, i.e.,  $\Theta = [\theta_{(0)}, \theta_{(\Delta t)}, \dots, \theta_{((K-1)\Delta t)}]$ . Using (13), the  $\Theta$  is expressed in matrix form as given in [30]

$$\Theta = \mathbf{B}\mathbf{v} + \epsilon \quad (14)$$

where  $\mathbf{B}$  is the precalculated matrix obtained from (13) and  $\mathbf{v} = [v_0 \ v_1 \ v_2]^T$ . The least square approach is used to calculate the vector  $\mathbf{v}$ , and hence, estimating the frequency and rate of change of frequency.

## III. COMPLIANCE TESTS

The performance analysis of proposed dictionary based phasor estimator (DDPE) is done as per the test requirements provided in IEEE C37.118.1a-2014 standard. The proposed DDPE algorithm is developed using MATLAB software to carry above standard tests in the Intel (R) Core 2 Duo processor at 3.00-GHz personal computer.

TABLE I  
SPECIFICATIONS OF COMPLIANCE TEST SIGNALS

Parameter	Notation	Specification
Nominal magnitude	$R_m$	150
Nominal frequency	$f_o$	50 Hz
Off-nominal frequency	$f$	$50 \pm 2$ Hz
Phase angle	$\theta$	$0 - 360^\circ$
Step size	$\mu$	$3.6^\circ$
Decaying dc component	$\Upsilon$	$30 - 90\%$
	$\tau$	$10 - 100$ ms
Gaussian noise (SNR)	$\mathcal{N}(0, \sigma^2)$	$15 - 50$ dB
Harmonic level	$R_2$	$1.33 - 6.667\%$
	$R_{k+1}$	$0.2R_k$
	$\theta_k$	$\theta/k$
Modulation level	$f_m$	$0.25 - 2.0$ Hz
	$K_x$	$\pm 0.1$
	$K_a$	$\pm \pi/18$
Frequency ramp rate	$R_f$	$\pm 1$ Hz/s
Step change	$K_x$	$\pm 0.1$
	$K_a$	$\pm \pi/18$
Frequency ramp rate	$R_f$	$\pm 1$ Hz/s

The presented work compares the proposed method, i.e., DDPE with some of recent and popular dynamic phasor estimators such as Hilbert transform-based dynamic phasor estimator (HDPE) [20], convolution-based dynamic phasor estimator (CDPE) [21], least square approximation-based dynamic phasor estimator (LDPE) [6], and Shank's dynamic phasor estimator (SDPE) [11]. To show the accuracy of estimated phasor by various methods, a well-known performance identifier widely used in the synchrophasor literature (15) called TVE is considered in the paper

$$\% \text{TVE} = \sqrt{\frac{(D_r^e - D_r^a)^2 + (D_i^e - D_i^a)^2}{(D_r^a)^2 + (D_i^a)^2}} \times 100 \quad (15)$$

where  $D_r^e$  and  $D_i^e$  are the real and imaginary quantities of an estimated phasor, and  $D_r^a$  and  $D_i^a$  are the real and imaginary quantities of an actual (true) phasor.

As per the test requirements of IEEE C37.118.1a-2014 standard, the following compliance test signals, such as: 1) decaying dc component signal; 2) electric noise signal; 3) off-nominal frequency signal; 4) modulated signal; 5) step change signal; and 6) frequency ramp rate signal are utilized to show the effectiveness of the proposed DDPE algorithm in estimating the phasor under various dynamic conditions. The specifications of test signals tabulated in Table I are utilized for performance evaluation of proposed DDPE and other algorithms.

The sampled data of a signal obtained with the sampling frequency of 1 kHz is been fed to the proposed DDPE algorithm along with other algorithms for estimation of phasor at a reporting rate of 50 frames per second. The observation window of one cycle, i.e., 20 ms, is considered for dynamic phasor estimation of a signal by the proposed technique, i.e., DDPE and other algorithms. The reporting rate of

50 frames per second is used in simulation, but in hardware, a reporting rate of 25 frames per second is used for estimating the phasors.

#### A. Decaying dc Component Test

The presence of decaying dc components in fault current is one of the challenging issues in synchrophasor estimation algorithms. Typically, the amplitude of dc components varies from 30% to 90%, and its time constant varies from 0.5 to 5 cycles depending on the fault resistance and network structure. The mathematical expression, as given in the following equation, is used to simulate the effect of the presence of decaying dc component in a signal:

$$r_1(t) = R_m \sin(2\pi f_o t + \theta) + \Upsilon e^{-t/\tau} \quad (16)$$

where  $\Upsilon$  and  $\tau$  are the magnitude and time constant of decaying dc component, respectively.

Several phasor estimation methods have been presented in the literature [22], [23] with decaying dc component and their effect on the estimated phasors. However, most of these methods have acceptable performance only for the specified values of decaying dc magnitude and time constant. In this paper, an investigation on the performance of the proposed DDPE algorithm with the variation of decaying dc magnitude ( $\Upsilon$ ), i.e., 30%–90%, and time constant ( $\tau$ ), i.e., 10–100 ms, has been carried out for a 50-Hz signal.

1) *Influence of Magnitude of dc Component*: In this case, the magnitude ( $\Upsilon$ ) of decaying dc component in (16) is varied from 30% to 90% with  $R_m = 150$ , time constant  $\tau = 30$  ms, nominal frequency  $f_o = 50$  Hz, and phase angle  $\theta = 10^\circ$  to test the phasor estimation performance of proposed DDPE algorithm.

Table II shows the impact of magnitude variation in decaying dc component on the sinusoidal signal, and it can be observed that the TVE values decline as decaying dc components die out. Interestingly, the TVE values of DDPE reduce to very low level, i.e., <1% after  $t = 80$  ms, for the magnitude variation of decaying dc component of the signal. The TVE values of DDPE at 80 ms during 30%, 50%, 70%, and 90% magnitudes are 0.327%, 0.544%, 0.762%, and 0.990%, respectively. It is worth noting that with the proposed DDPE, only one of the calculated phasor at 70% and 90% has higher TVE value, but others are either close or less than the acceptable value of TVE, i.e.,  $\leq 3\%$ .

2) *Influence of Time Constant*: In this case, the time constant ( $\tau$ ) of decaying component in (16) is varied from 10 to 100 ms with  $R_m = \Upsilon = 150$ ,  $f_o = 50$  Hz, and  $\theta = 10^\circ$  to evaluate the performance of proposed DDPE algorithm. Table III shows the simulation results in terms of estimate magnitude and % TVE, respectively, by proposed DDPE technique with the presence of decaying dc component in the signal.

From Table III, it is observed that the estimated phasor, at time  $t = 0.02$  s, is more affected by the presence of dc components, but the TVE of the subsequent phasor are close to 3%. Moreover, it is observed that the time required to achieve the TVE value below 3% is proportional to the time

TABLE II

ESTIMATED MAGNITUDE AND TVE OF (16) WITH  $\Upsilon$  VARIATIONS

Time(s)	$\Upsilon$ variations in (%)			
	30	50	70	90
0.02	153.619 2.428%	156.033 4.042%	158.446 5.656%	160.860 7.271%
0.04	151.858 1.247%	153.097 2.070%	154.336 2.903%	155.575 3.727%
0.06	150.954 0.636%	151.590 1.069%	152.226 1.491%	152.862 1.913%
0.08	150.490 0.327%	150.816 0.544%	151.143 0.762%	151.469 0.990%
0.10	150.251 0.168%	150.419 0.280%	150.587 0.391%	150.754 0.503%
0.12	150.129 0.087%	150.215 0.144%	150.301 0.201%	150.387 0.259%
0.14	150.066 0.046%	150.110 0.075%	150.155 0.104%	150.199 0.133%
0.16	150.034 0.027%	150.057 0.040%	150.079 0.055%	150.102 0.069%
0.18	150.017 0.018%	150.029 0.024%	150.041 0.031%	150.052 0.038%
0.20	150.009 0.015%	150.015 0.017%	150.021 0.020%	150.027 0.023%
0.22	150.005 0.014%	150.008 0.015%	150.011 0.016%	150.014 0.017%
0.24	150.002 0.014%	150.004 0.014%	150.006 0.014%	150.007 0.015%
0.26	150.001 0.014%	150.002 0.014%	150.003 0.014%	150.004 0.014%
0.28	150.001 0.014%	150.001 0.014%	150.001 0.014%	150.002 0.014%
0.30	150.000 0.014%	150.001 0.014%	150.001 0.014%	150.001 0.014%

constant ( $\tau$ ) of decaying component, i.e., at  $\tau = 10$ , the time required for TVE less than 3% is 0.04 s, similarly at  $\tau = 30$ , it is 0.06 s, and at  $\tau = 60$  and 100, it is 0.08 s. Thus, it is observed that the TVE accuracy of proposed DDPE depends on the value of time constant of decaying dc component, e.g., for high value of  $\tau$ , more time is required to achieve the TVE below 3%.

### B. Electric Noise Tests

Electric noise with wide spectral content lower than 200 kHz is undesirable in power system electrical signals (*voltage/current*). The faulty connections in various equipments, power converters, control circuits, capacitor banks operation, transmission/distribution lines, etc., are the major sources of noise in the power signals.

Based on the sources of the noise, the harmonic noise and random noise are considered in this paper.

1) *Harmonic Distortion Test*: The fundamental sinusoidal signal of 50-Hz frequency along with its harmonics [ $\leq 10$ ] having a mathematical model as given in the following equation is considered in this paper for showing the effectiveness of various methods in estimation of phasor in the presence of harmonics:

$$r_2(t) = R_m \sin(2\pi f_{ot} t + \theta) + \sum_{k=2}^{10} R_k \sin(2\pi k f_{ot} t + \theta_k) \quad (17)$$

where  $k$  is the harmonic order,  $R_k$  and  $\theta_k$  are the peak amplitude and phase angle of the harmonic signal

TABLE III

ESTIMATED MAGNITUDE AND TVE OF (16) WITH  $\tau$  VARIATIONS

Time(s)	$\tau$ variations in (ms)			
	10	30	60	100
0.02	155.394 3.743%	162.067 8.072%	159.800 6.539%	157.147 4.764%
0.04	150.729 0.506%	156.195 4.149%	157.022 4.683%	155.851 3.901%
0.06	150.099 0.067%	153.180 2.125%	155.031 3.357%	154.791 3.194%
0.08	150.013 0.017%	151.633 1.097%	153.605 2.408%	153.922 2.615%
0.10	150.002 0.014%	150.838 0.559%	152.583 1.722%	153.211 2.141%
0.12	150.000 0.014%	150.430 0.287%	151.851 1.234%	152.629 1.753%
0.14	150.000 0.014%	150.221 0.148%	151.326 0.884%	152.153 1.435%
0.16	150.000 0.014%	150.113 0.077%	150.950 0.634%	151.762 1.175%
0.18	150.000 0.014%	150.058 0.041%	150.681 0.454%	151.443 0.962%
0.20	150.000 0.014%	150.030 0.024%	150.488 0.326%	151.181 0.788%
0.22	150.000 0.014%	150.015 0.017%	150.350 0.233%	150.967 0.645%
0.24	150.000 0.014%	150.008 0.015%	150.250 0.168%	150.792 0.528%
0.26	150.000 0.014%	150.004 0.014%	150.179 0.120%	150.648 0.432%
0.28	150.000 0.014%	150.002 0.014%	150.129 0.087%	150.531 0.354%
0.30	150.000 0.014%	150.001 0.014%	150.092 0.063%	150.435 0.290%

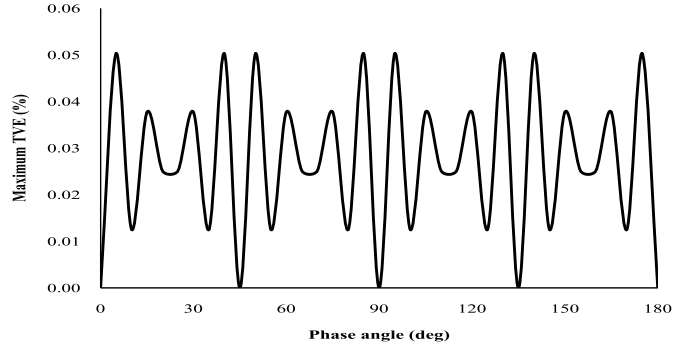


Fig. 1. Maximum TVE under different harmonic levels for DDPE.

The accuracy of estimated phasor as given in term of TVE for the signal as given in (17) is shown in Fig. 1 with the phase angle varying from  $0^\circ$  to  $180^\circ$ , and harmonic level of the second component varying from 1.33% to 6.67% of fundamental amplitude ( $R_m$ ). From Fig. 1, the results describe that the TVE varies periodically with maximum TVE of 0.057% in the presence of harmonics in the fundamental sinusoidal signal. It is also observed that the TVE is 0% at  $0^\circ$ ,  $45^\circ$ ,  $90^\circ$ ,  $135^\circ$ , and  $180^\circ$  phase angles. Furthermore, the variation of harmonic levels in the signal (17) does not affect the TVE and is constant at different harmonic levels.

A signal (17) corrupted by harmonics [ $\leq 10$ ] of variable level [5.0%] with a phase angle,  $\theta = 10^\circ$  is considered to compare the performance of proposed DDPE with other phasor estimation algorithms. The TVE of different methods

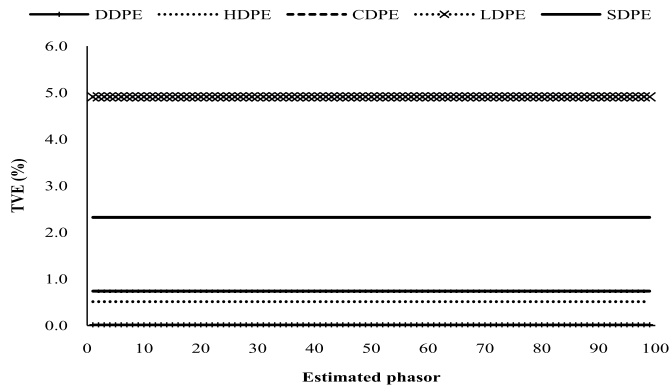


Fig. 2. TVE under harmonics in sinusoidal signal (17).

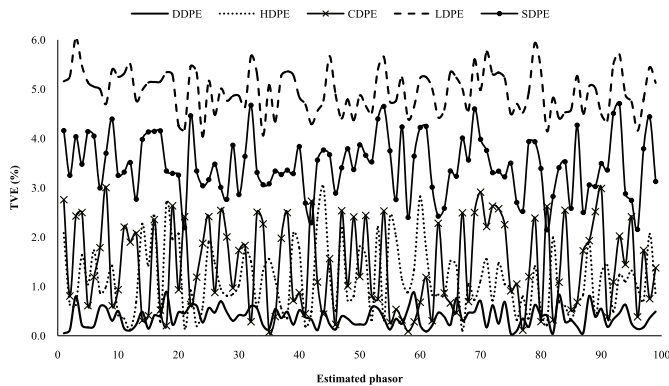


Fig. 3. TVE under sinusoidal signal corrupted with Gaussian noise (18).

during phasor estimation of signal (17) is shown in Fig. 2. The TVE results point out that TVE of SDPE (2.32%) and LDPE (4.98%) is more than that of proposed DDPE (0.014%). Whereas, the TVE of CDPE (0.85%) and HDPE (0.62%) is less than 1% according to the standard [27], and is also more than that of DDPE. From Fig. 2, the TVE of DDPE is nearly zero which reveals that the proposed DDPE can accurately estimate the fundamental component phasor of a measured signal in the presence of harmonics.

2) *Random Noise Test*: The additive Gaussian random noise with the sinusoidal signal of 50-Hz frequency is considered as another test signal and its mathematical representation is given as

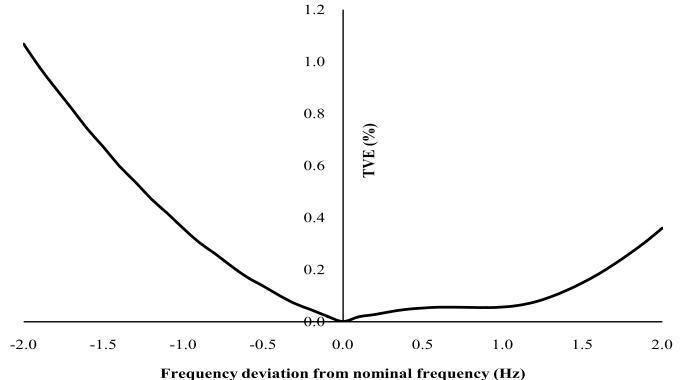
$$r_3(t) = R_m \sin(2\pi f_o t + \theta) + \mathcal{N} \quad (18)$$

where  $\mathcal{N}$  is a Gaussian noise present in the signal.

A sinusoidal signal with SNR of 10.5 dB as defined in (18) is used to know the effect of noise on the various estimation algorithms during computation of phasor [24]. The accuracy in terms of TVE of different phasor estimation algorithms is shown in Fig. 3. The results describe that the average TVE of LDPE (5.17%) and SPDE (3.61%) is greater than 3%, whereas for CDPE (1.83%) and HDPE (1.75%), it varies between 1.5% and 3%. From Fig. 3, the average TVE of DDPE (0.42%) is less than 1% which shows that the proposed DDPE can effectively estimate the fundamental component phasor of a signal in the presence of Gaussian noise.

TABLE IV  
TVE UNDER THE INFLUENCE OF NOISE

SNR (dB)	Maximum TVE (%)				
	DDPE	HDPE	CDPE	LDPE	SDPE
15	1.2941	2.4401	2.9734	5.8149	4.7588
30	0.5942	1.1045	1.7061	3.3197	2.0517
50	0.1874	0.5492	0.9175	1.8055	1.2769

Fig. 4. TVE of nominal frequency sinusoidal signal at  $R_m = 150$  and  $\theta = 10^\circ$  with different frequency deviations for DDPE.

Furthermore, an investigation is carried on DDPE and other algorithms to test their performance under the influence of noise at  $\theta = 15^\circ$ . Table IV shows the performance of DDPE and other techniques in terms of maximum TVE during SNR of 15–50 dB variations [24], [25]. It can be observed that the proposed DDPE algorithm achieves much better accuracy (low TVE) than that of HDPE, CDPE, LDPE, and SDPE algorithms. Thus, it is worth noting that the proposed DDPE algorithm is immune to noise during phasor estimation of a signal.

### C. Off-Nominal Frequency Test

This section investigates the effect of off-nominal frequencies on the proposed algorithm. In most of the practical power grids, typically the frequency is kept close to its nominal value with deviation not more than  $\pm 3\%$ . The model used in the simulation is expressed as

$$r_4(t) = R_m \sin(2\pi f t + \theta) = R_m \sin(2\pi f_o t + \theta(t)) \quad (19)$$

where  $f$  is an off-nominal frequency and  $f = f_o + \Delta f$ ,  $\Delta f$  is the frequency deviation from nominal frequency ( $f_o$ ).

In this section, the measurement accuracy of proposed DDPE is evaluated on signal (19) with the frequency deviations ( $\Delta f$ ) of  $\pm 2$  Hz for a signal with 50 Hz as the nominal frequency. The performance of proposed DDPE algorithm in terms of TVE is shown in Fig. 4, with the frequency of the fundamental component changed in steps of 0.1 Hz. It is observed from Fig. 4 that the measurement accuracy of proposed DDPE algorithm is more sensitive for frequencies less than nominal frequency ( $f_o$ ), i.e., TVE at  $\Delta f = -2$  Hz is 1.067%, whereas its performance is much better for the

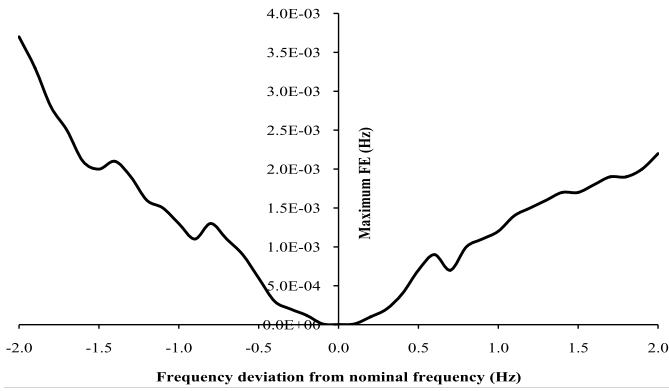


Fig. 5. Maximum FE of nominal frequency sinusoidal signal at  $R_m = 150$  and  $\theta = 10^\circ$  with different frequency deviations for DDPE.

frequencies more than the nominal frequency ( $f_0$ ), i.e., TVE at  $\Delta f = 2$  Hz is 0.361%. Moreover, the TVE of proposed DDPE algorithm is less than 3% as per [27] under frequency deviations upto  $\pm 2$  Hz. Furthermore, the maximum frequency error (FE) achieved by proposed DDPE is shown in Fig. 5, which is well within the requirements of [27], i.e., 0.005 Hz. Thus, the simulation results reveal that the DDPE can able to accurately estimate the dynamic phasor and frequency of a signal during off-nominal frequency conditions.

#### D. Modulation Test

The stressed tie-lines, bulk load changes, alternator outages, and transmission line faults are responsible for rotor angle oscillations in synchronous machines which may result into power swings in the system. Such power swings may cause the mal-operation of the protective relays in the transmission networks, and hence, can lead toward the cascaded outages of lines and system blackouts. Generally, power swings can be mathematically represented as the modulated sinusoidal signal as given in the following equation:

$$r_5(t) = R_m(1 + K_x \sin(2\pi f_m t + \theta)) \times \sin(2\pi f_{ot} t + K_a \sin(2\pi f_m t) + \theta) \quad (20)$$

where  $K_x$  and  $K_a$  are the modulated amplitude and phase coefficients respectively, and  $f_m$  is the modulation frequency

The effectiveness of proposed DDPE in estimating the phasor during power swing is tested with the help of amplitude and phase modulated signal (20) by varying phase angle from  $0^\circ$  to  $180^\circ$  and modulation frequency  $f_m$  from 0.25 to 2 Hz, simultaneously. The accuracy of proposed DDPE algorithm in terms of TVE during phasor (i.e., magnitude and phase angle) estimation of signal (20) is shown in Fig. 6.

From Fig. 6, it is observed that the TVE of DDPE slightly increases from  $0^\circ$  to  $90^\circ$  and then decreases from  $90^\circ$  to  $180^\circ$ . At low modulation frequencies, the TVE of proposed DDPE is nearly constant with variation in phase angle of a signal. It is also noticed that as the modulation frequency of signal (20) increasing, the TVE of proposed DDPE also increases and hits a maximum TVE of 1.98% at  $90^\circ$  in the presence of 2-Hz modulation frequency signal which is less than 3% as defined by the standard [27] for PMU.

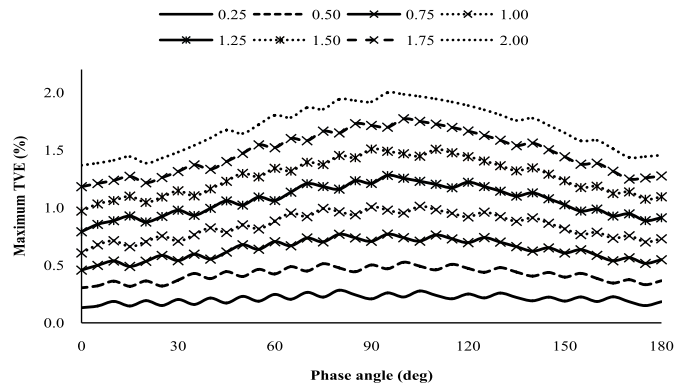


Fig. 6. Maximum TVE of amplitude and phase modulated signal with different  $f_m$  and  $\theta$  from  $0^\circ$  to  $180^\circ$  for DDPE.

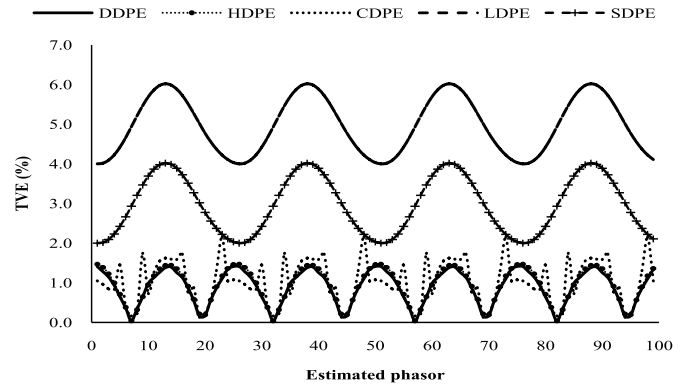


Fig. 7. TVE under amplitude and phase-modulated signal (20).

The time-shifted nonoverlapping window data of signal (20) is given to different algorithms for estimation of phasors. The effectiveness of phasor estimation algorithms in terms of TVE is compared and depicted in Fig. 7. It is observed from the results that the maximum TVE of proposed DDPE (1.42%) is much lower than that of LDPE (6.11%) and SDPE (3.89%). The TVE of DDPE algorithm is highly competitive with HDPE method and is slightly on lower side, whereas the performance of DDPE method is better than CDPE as shown in Fig. 7. Thus, from above-mentioned comparative results, the proposed DDPE algorithm can effectively estimate the phasor of a complex modulated signal in the power systems during disturbances.

#### E. Step Change Test

During faults, the voltage or current transients are observed in the transmission network due to sudden change in the impedance and the configuration of power network. A signal which represents these transients is mathematically modeled as (21) and is used for the comparative analysis of different phasor estimation algorithms

$$r_6(t) = R_m(1 + K_x U_1(t)) \sin(2\pi f_{ot} t + K_a U_1(t) + \theta) \quad (21)$$

where  $K_x$  and  $K_a$  are the modulated magnitude and phase coefficients,  $\theta = 15^\circ$ ,  $U_1(t)$  is the unit step function and is

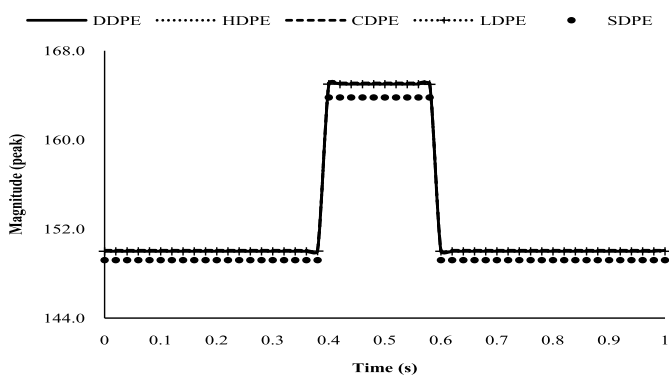


Fig. 8. Estimated magnitude of step-change signal (21).

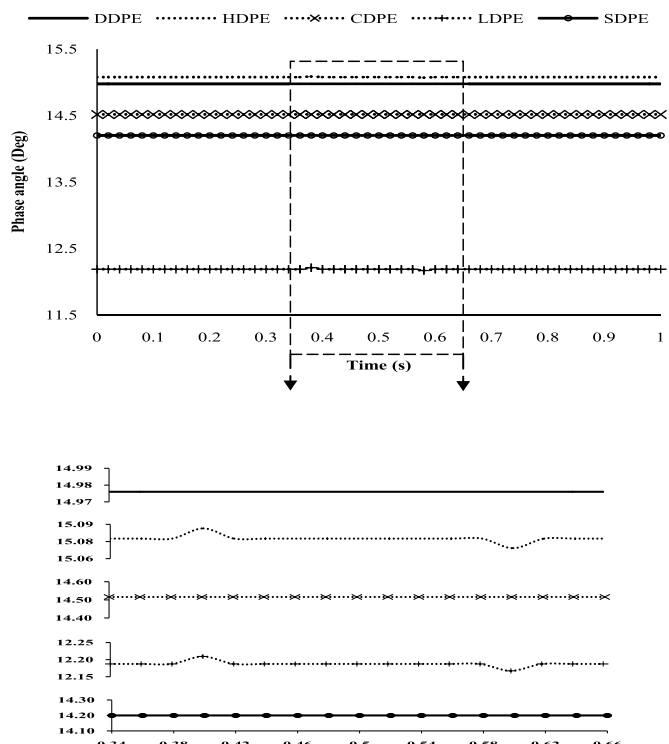


Fig. 9. Estimated phase angle of step-change signal (21)

defined by

$$U_1(t) = \begin{cases} 0, & \text{if } t < t_1 \\ 1, & \text{if } t > t_1 \end{cases} \quad (22)$$

where  $t_1$  is the time when the step change is applied.

As per the requirements of IEEE C37.118.1a-2014 standard [28], a step increase and decrease in magnitude of 10% occurred at  $t = 0.4$  and  $0.6$  s, respectively, in signal (21). This simulated test signal is given to various estimation algorithms for phasor computation and their effectiveness is compared.

It is observed from Fig. 8 that above all algorithms have accurately estimated the varied magnitude at  $t = 0.4$  and  $0.6$  s except SDPE algorithm.

From Fig. 9, it can be observed that the estimation of phase angle by DDPE ( $14.976^\circ$ ) is accurate as compared with that of HDPE ( $15.087^\circ$ ), CDPE ( $14.500^\circ$ ), LDPE ( $12.223^\circ$ ), and

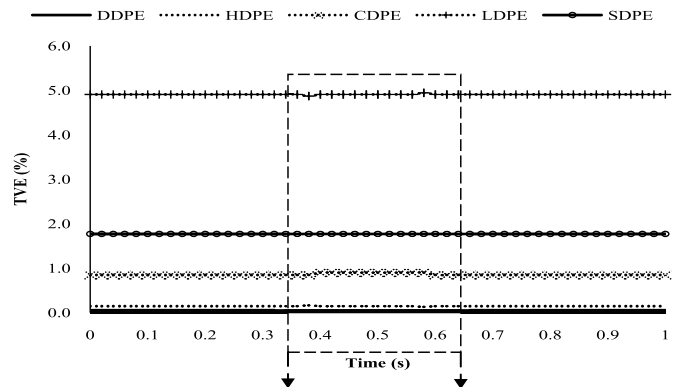
Fig. 10. Instantaneous TVE under step-change at  $t = 0.4$  and  $0.6$  s.

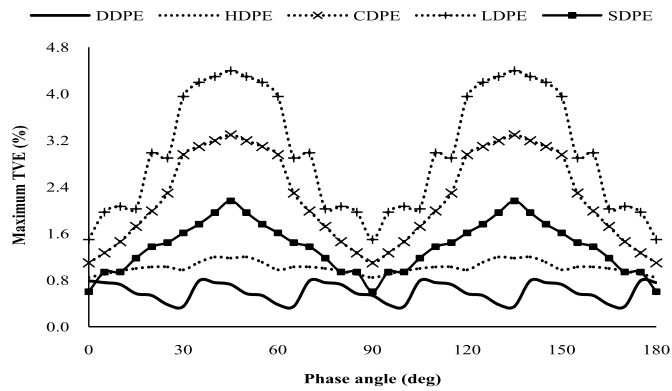
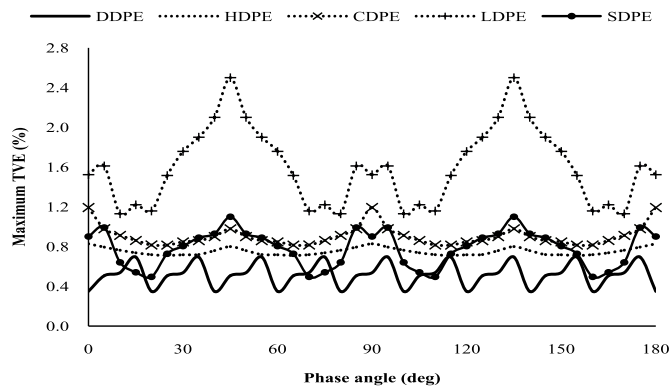
TABLE V  
RESPONSE TIMES UNDER STEP TEST

Algorithm	Response Time (ms)	
	$K_x = 10\%$	$K_a = 10^\circ$
DDPE	25	29
HDPE	31	36
CDPE	42	48
LDPE	38	42
SDPE	28	33

SDPE ( $14.200^\circ$ ). The working performance of each phasor estimation algorithm is clearly visualized by TVE, which is shown in Fig. 10. Thus, the proposed DDPE algorithm with nearly zero TVE under transients can effectively detect the sharp variations in a signal and accurately identify the faults in the power system.

Furthermore, the response time for P-class PMU to be fast during step changes in the estimated signal. The IEEE Standards Committee released IEEE C37.118.1a-2014 where the response time in the step test for P-class PMU is  $2/f_0$ , i.e., 40 ms. A signal (21) with step change of 10% and  $10^\circ$  in magnitude and phase angle, respectively, is fed to the proposed DDPE and other algorithms. The performance in terms of response time of algorithms during step changes is given in Table V.

The simulation results as depicted in Table V reveal that the response time of DDPE is lower than that of other dynamic phasor estimation techniques. Thus, the proposed DDPE algorithm is suitable for P-class PMU in power system protection applications according to IEEE Synchrophasor standard [28].

Fig. 11. Maximum TVE under  $+1 \text{ Hz/s}$  frequency ramp rate for DDPE.Fig. 12. Maximum TVE under  $-1 \text{ Hz/s}$  frequency ramp rate for DDPE.

#### F. Frequency Ramp Test

The multivalve operation of steam turbines in large power generating station during automatic generation control results in frequency ramps for short period in the power system signals. The linear shift in frequency of a sinusoidal signal is mathematically represented as

$$r_f(t) = R_m \sin(2\pi f_0 t + (\pi R_f t^2) + \theta) \quad (23)$$

where  $R_f$  is the frequency ramp rate in Hz/s

A sinusoidal signal (23) with ramp rate of  $\pm 1 \text{ Hz/s}$  (as per standard [27]) at varied phase angles from  $0^\circ$  to  $180^\circ$  is given to different estimation algorithms for phasor measurement. It is observed that the TVE signature of proposed DDPE algorithm during phasor estimation of (23) is periodic  $\mp$  saw-tooth with change in phase angle from  $0^\circ$  to  $180^\circ$  at  $\pm 1\text{-Hz/s}$  ramp rate, respectively, and shown in Figs. 11 and 12, respectively. At phase angles  $15^\circ$ ,  $65^\circ$ ,  $70^\circ$ , and  $115^\circ$ , the TVE of DDPE algorithm is slightly higher than that of SDPE. Whereas, at other phase angles, the performance of DDPE is better than SDPE as shown in Fig. 12. The maximum TVE of DDPE algorithm is less than 1% and slightly varies with phase angle variations. Thus, the proposed DDPE algorithm can effectively estimate the phasor of a signal that consists of  $\pm 1\text{-Hz/s}$  frequency ramp rates.

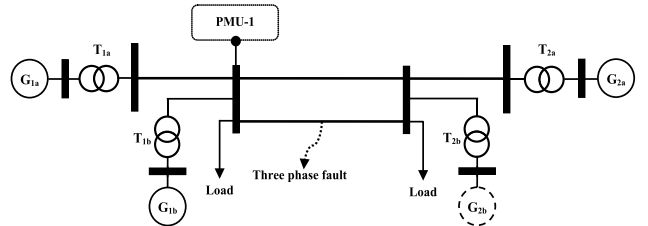


Fig. 13. Modified two-area test power system.

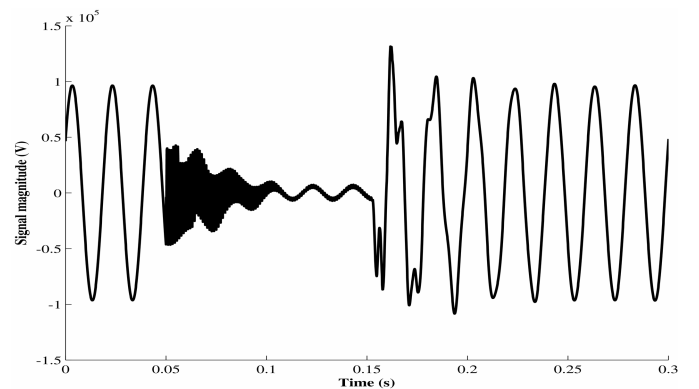


Fig. 14. Voltage waveform at bus 1.

#### IV. MODIFIED TWO-AREA POWER SYSTEM TEST CASE

A modified two-area power system as provided in [20], [29] with one of the generator replaced by an equivalent doubly fed induction generator (DFIG) is shown in Fig. 13 with a dotted circle. The system is simulated over PSS/E/Sincal with the WT3G1 used as the dynamic model for DFIG.

The PMU-1 located at the one end of the transmission line, as shown in Fig. 13, uses sample values of bus voltage and line current of a line with a three-phase fault initiated at 50 ms, and the fault is subsequently cleared after a duration of 100 ms. The waveform of voltage and current samples utilized for the comparative analysis of the proposed method with other methods are shown in Figs. 14 and 15, respectively.

The estimated phasors by proposed DDPE method and other algorithms for bus voltage during prefault (i.e., at  $t = 0.02 \text{ s}$ , estimated phasor =  $96.758 \angle 28.17^\circ$ ; at  $t = 0.04 \text{ s}$ , estimated phasor =  $96.758 \angle 28.17^\circ$ ), three phase fault (i.e.,  $t = 0.06, 0.08, \dots, 0.14 \text{ s}$ ) and postfault (i.e.,  $t = 0.16, \dots, 0.22 \text{ s}$ ) is provided in Table VI. The table also includes the calculated or the true value of phasor magnitude. Similarly, the estimate phasors of a line current during prefault, three phase fault, and postfault conditions are given in Table VII.

From the estimated phasors corresponding to line voltage and current, as tabulated in Tables VI and VII, it can be observed that the estimated phasors by the proposed method (DDPE) is more accurate (in terms of TVE) as compared with other methods during prefault, during fault, and postfault conditions. Thus, the accurate and fast phasor estimation of proposed DDPE algorithm suits for protection applications in power system/distribution grids.

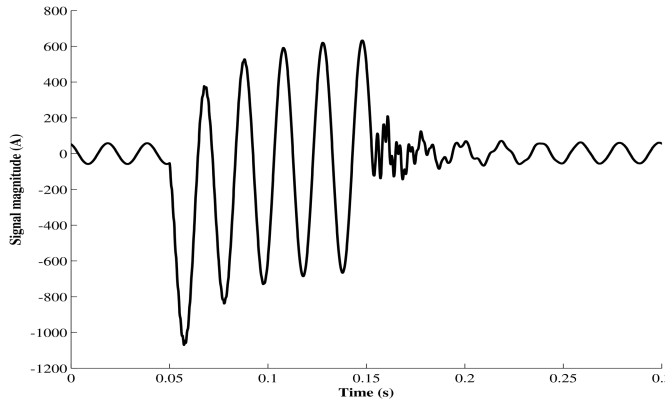


Fig. 15. Current waveform at bus 1.

TABLE VI  
ESTIMATED VOLTAGE PHASOR (kV) BY (PMU-1)

Time(s)	True	DDPE	HDPE	CDPE	LDPE	SDPE
0.02	96.760	96.758	96.763	96.763	96.589	97.142
	$\angle 28.12^\circ$	$\angle 28.17^\circ$	$\angle 28.65^\circ$	$\angle 28.78^\circ$	$\angle 25.87^\circ$	$\angle 30.87^\circ$
0.04	96.760	96.758	96.763	96.763	96.589	97.142
	$\angle 28.12^\circ$	$\angle 28.17^\circ$	$\angle 28.65^\circ$	$\angle 28.78^\circ$	$\angle 22.99^\circ$	$\angle 25.99^\circ$
0.06	6.512	6.521	6.472	6.276	4.597	5.213
	$\angle 183.7^\circ$	$\angle 182.9^\circ$	$\angle 174.1^\circ$	$\angle 167.5^\circ$	$\angle 148.1^\circ$	$\angle 154.1^\circ$
0.08	6.512	6.517	6.398	6.289	9.135	5.631
	$\angle 183.7^\circ$	$\angle 182.7^\circ$	$\angle 178.6^\circ$	$\angle 170.2^\circ$	$\angle 149.8^\circ$	$\angle 167.6^\circ$
0.10	6.512	6.511	6.215	6.172	9.135	5.743
	$\angle 183.7^\circ$	$\angle 181.0^\circ$	$\angle 178.1^\circ$	$\angle 174.0^\circ$	$\angle 132.0^\circ$	$\angle 142.1^\circ$
0.12	6.512	6.500	6.435	6.309	7.746	5.746
	$\angle 183.7^\circ$	$\angle 183.0^\circ$	$\angle 178.1^\circ$	$\angle 174.5^\circ$	$\angle 162.8^\circ$	$\angle 172.5^\circ$
0.14	6.512	6.507	6.318	6.309	7.746	5.746
	$\angle 183.7^\circ$	$\angle 182.5^\circ$	$\angle 178.6^\circ$	$\angle 170.0^\circ$	$\angle 160.0^\circ$	$\angle 169.2^\circ$
0.16	96.760	101.241	105.639	105.639	100.173	80.173
	$\angle 28.12^\circ$	$\angle 29.53^\circ$	$\angle 32.78^\circ$	$\angle 33.27^\circ$	$\angle 22.94^\circ$	$\angle 37.17^\circ$
0.18	96.760	96.756	96.494	96.494	95.195	95.195
	$\angle 28.12^\circ$	$\angle 27.67^\circ$	$\angle 27.84^\circ$	$\angle 27.93^\circ$	$\angle 25.31^\circ$	$\angle 30.87^\circ$
0.20	96.760	96.572	97.470	97.470	97.061	97.061
	$\angle 28.12^\circ$	$\angle 28.06^\circ$	$\angle 28.03^\circ$	$\angle 29.84^\circ$	$\angle 25.89^\circ$	$\angle 33.87^\circ$
0.22	96.760	96.672	96.692	96.692	96.467	96.467
	$\angle 28.12^\circ$	$\angle 28.01^\circ$	$\angle 27.96^\circ$	$\angle 28.98^\circ$	$\angle 25.97^\circ$	$\angle 33.87^\circ$

Furthermore, an interleave analysis is performed with a general reporting time  $t_r = 20$  ms, the reporting interval  $T = 20$  ms, and  $p = 4$  is the number of test performed, i.e., interleave analysis with four windows as per the IEEE

TABLE VII  
ESTIMATED CURRENT PHASOR (A) BY (PMU-1)

Time(s)	True	DDPE	HDPE	CDPE	LDPE	SDPE
0.02	60.475	59.673	58.373	58.372	48.025	57.995
	$\angle 110.0^\circ$	$\angle 111.4^\circ$	$\angle 113.6^\circ$	$\angle 107.6^\circ$	$\angle 111.1^\circ$	$\angle 105.8^\circ$
0.04	60.475	59.673	58.373	58.372	48.025	57.995
	$\angle 110.0^\circ$	$\angle 111.4^\circ$	$\angle 113.6^\circ$	$\angle 104.0^\circ$	$\angle 111.1^\circ$	$\angle 105.2^\circ$
0.06	650.000	690.190	700.502	706.509	560.063	580.483
	$\angle 240.0^\circ$	$\angle 255.4^\circ$	$\angle 260.0^\circ$	$\angle 272.5^\circ$	$\angle 119.0^\circ$	$\angle 120.8^\circ$
0.08	650.000	655.167	659.658	659.671	634.416	641.665
	$\angle 240.0^\circ$	$\angle 272.1^\circ$	$\angle 298.3^\circ$	$\angle 151.1^\circ$	$\angle 142.1^\circ$	$\angle 180.6^\circ$
0.10	650.000	650.249	649.150	649.163	703.408	644.372
	$\angle 240.0^\circ$	$\angle 300.3^\circ$	$\angle 303.6^\circ$	$\angle 129.6^\circ$	$\angle 123.5^\circ$	$\angle 165.9^\circ$
0.12	650.000	650.201	648.798	648.801	581.148	634.561
	$\angle 241.0^\circ$	$\angle 301.7^\circ$	$\angle 305.7^\circ$	$\angle 130.5^\circ$	$\angle 124.0^\circ$	$\angle 200.3^\circ$
0.14	650.000	480.117	489.307	489.303	600.438	583.507
	$\angle 240.0^\circ$	$\angle 119.7^\circ$	$\angle 120.6^\circ$	$\angle 125.7^\circ$	$\angle 126.2^\circ$	$\angle 190.6^\circ$
0.16	60.475	80.174	82.395	82.391	98.433	100.433
	$\angle 110.0^\circ$	$\angle 105.1^\circ$	$\angle 98.0^\circ$	$\angle 130.5^\circ$	$\angle 120.0^\circ$	$\angle 100.7^\circ$
0.18	60.475	7.842%	8.309%	9.591%	15.87%	12.431%
	$\angle 110.0^\circ$	$\angle 114.3^\circ$	$\angle 115.4^\circ$	$\angle 104.6^\circ$	$\angle 130.3^\circ$	$\angle 122.8^\circ$
0.20	60.475	60.509	63.495	63.487	54.719	64.926
	$\angle 110.0^\circ$	$\angle 110.2^\circ$	$\angle 109.1^\circ$	$\angle 100.1^\circ$	$\angle 120.0^\circ$	$\angle 117.4^\circ$
0.22	60.475	58.561	57.619	57.617	56.067	56.754
	$\angle 110.0^\circ$	$\angle 115.1^\circ$	$\angle 116.1^\circ$	$\angle 118.4^\circ$	$\angle 121.7^\circ$	$\angle 115.8^\circ$

Synchrophasor standard, to get intermediate phasors to better understand the performance of proposed DDPE algorithm. The above-mentioned interleave analysis is carried on the simulated voltage and current signals as shown in Figs. 14 and 15, respectively. The results of interleave analysis, in terms of TVE, are shown in Figs. 16 and 17, respectively. As the accuracy requirements under the transient condition are not a part of IEEE C37.118.1a-2014 standard, but still we can observe that TVE of the estimated voltage phasor is less than 5%, whereas the TVE of the estimated current phasor is less than 9% during fault [26]. Thus, we can say that the proposed DDPE algorithm is suitable for P-class PMU to respond during rapid variations (transients) in smart electric grids.

## V. HARDWARE VERIFICATION OF DEVELOPED PMU

The above-mentioned IEEE standard [27] compliance tests clearly explain that the proposed DDPE approach can accurately estimate the fundamental component phasor of a signal during different transient or dynamic conditions. Section II of this paper states that the proposed DDPE approach is simple

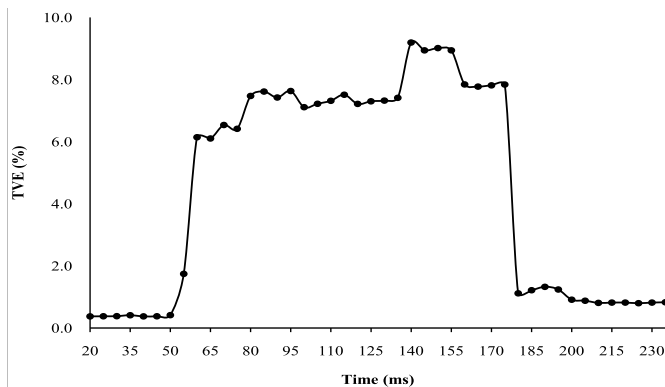


Fig. 16. TVE of estimated voltage phasor (Fig. 14) after interleave analysis.

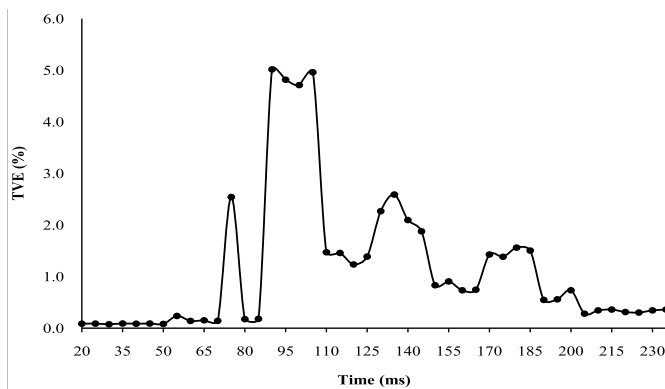


Fig. 17. TVE of estimated current phasor (Fig. 15) after interleave analysis.

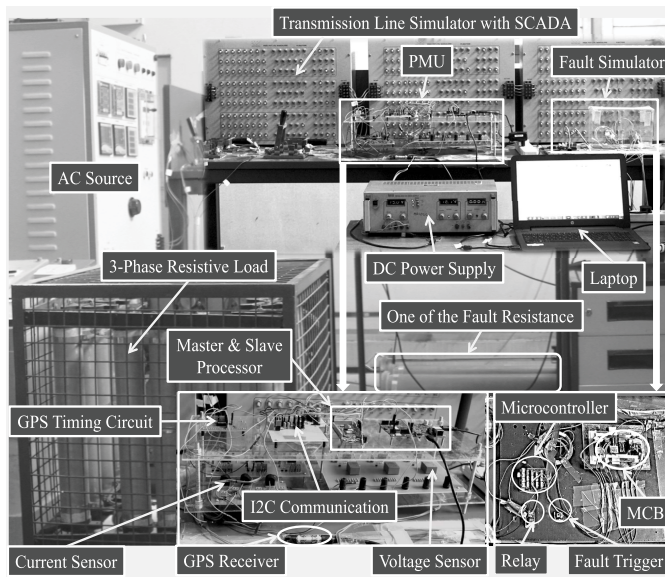


Fig. 18. Experimental setup for hardware verification of developed PMU.

in implementation and has less complexity to compute the phasor of a dynamic signal, accurately. The above major merits of proposed phasor estimation algorithm (DDPE) motivated to develop a hardware prototype of P-class PMU using cost effective components/devices/controllers.

The experimental setup, as shown in Fig. 18, includes a PMU prototype developed in the laboratory and a transmission line simulator. The corresponding single line diagram is

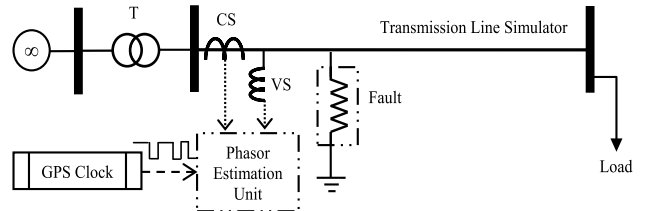


Fig. 19. Schematic of experiment setup model in the laboratory.

TABLE VIII  
EXPERIMENTAL SETUP PARAMETERS

Equipment	Specification
Grid supply ( $\infty$ )	415 V, 50 Hz, India's North-Eastern Grid
Transformer ( $T$ )	3 $\phi$ , 415 V/110 V
Current sensor ( $CS$ )	5 A, Hall effect, ACS712
Voltage sensor ( $VS$ )	10 – 500 V, 10 mA, Hall effect, LV25
Master-Slave Processor	Intel Galileo Gen vr.2, Arduino Due
GPS Clock	SEL-2407 model
DC power supply	$\pm 15$ V, APIlab
Microcontroller	Arduino UNO R3 board with ATmega 328
Relay	HSLS82, 15 A, 120 VAC
Fault	3 $\phi$ , resistive, star connected, 25 $\Omega$ distance-33%, duration-200 ms
Transmission line	400 kV, Twin Moose, 3 $\pi$ -sections 120 km, $R = 0.207$ , $X_L = 6.684 \Omega/\text{sect}$ $X_C = 1.2432 \Omega/\text{sect}$ , at 110 V level
Load	3 $\phi$ , resistive, star connected, 351 $\Omega$

shown in Fig. 19. The detailed specifications of developed experimental setup are provided in Table VIII.

The transmission line simulator consists of 3  $\pi$ -sections (i.e., each  $\pi$  section represents a 40-Km line) connected in series representing a 400-kV, 120-km transmission line. The analog simulator used has a base voltage of 110 V, which is equivalent to 400 kV for actual system and the base current of 1 A is equivalent 577 A of current for the actual system. With the use of fault simulator, a three-phase fault with fault resistance of 20  $\Omega$  is initiated for period of 0.1 s. The fault is located at a distance of 33% from grid end (i.e., from load) as shown in Fig. 19 [20].

Voltage and current sensors are located close to the grid busbar, i.e., just after the transformer as shown in Fig. 19, to measure the system voltage and current signals, respectively. The measured samples are provided to the low cost P-class PMU prototype developed in laboratory for verifying the suitability of the algorithm in estimating the phasor by utilizing low-cost hardware. Here, in the developed PMU prototype, the voltage and current signals are sampled at a rate of 10 samples per cycle by using inbuilt ADC of Arduino Due board with clock speed of 80 MHz and are provided to the proposed phasor estimation algorithm (DDPE) running on master processor through I2C communication. The resolution of inbuilt ADC of Arduino Due board is 10 bits. The power quality indices, i.e., SNR and total harmonic distortion of acquired voltage and current signals from experimental radial network,

TABLE IX

ESTIMATED PHASORS BY LAB SCALE PMU PROTOTYPE, WHERE "X" TO BE REPLACE BY "286.11.15.36" TO GET ACTUAL IST TIME

IST	Voltage (V)			Current (A)		
	True	Estimated	TVE	True	Estimated	TVE
X.200	115 $\angle 33.40^\circ$	115.14 $\angle 33.28^\circ$	0.24%	0.70 $\angle 53.15^\circ$	0.71 $\angle 53.24^\circ$	1.44%
X.240	115 $\angle 32.02^\circ$	115.14 $\angle 32.12^\circ$	0.21%	0.70 $\angle 51.77^\circ$	0.69 $\angle 51.94^\circ$	1.46%
X.280	115 $\angle 30.65^\circ$	115.13 $\angle 30.40^\circ$	0.45%	0.70 $\angle 50.40^\circ$	0.71 $\angle 50.64^\circ$	1.49%
X.320	115 $\angle 29.27^\circ$	115.13 $\angle 28.96^\circ$	0.55%	0.70 $\angle 49.02^\circ$	0.71 $\angle 49.12^\circ$	1.44%
X.360	115 $\angle 27.90^\circ$	115.13 $\angle 27.16^\circ$	1.30%	0.70 $\angle 47.65^\circ$	0.69 $\angle 47.42^\circ$	1.48%
X.400	110 $\angle 25.38^\circ$	110.70 $\angle 26.04^\circ$	1.32%	4.24 $\angle 18.38^\circ$	4.39 $\angle 18.72^\circ$	3.59%
X.440	110 $\angle 24.00^\circ$	110.23 $\angle 24.16^\circ$	1.09%	4.24 $\angle 17.00^\circ$	4.31 $\angle 17.44^\circ$	1.82%
X.480	110 $\angle 22.63^\circ$	109.61 $\angle 23.20^\circ$	1.05%	4.24 $\angle 15.63^\circ$	4.28 $\angle 16.02^\circ$	1.16%
X.520	110 $\angle 21.25^\circ$	110.84 $\angle 22.48^\circ$	2.29%	4.24 $\angle 14.25^\circ$	4.25 $\angle 14.64^\circ$	0.72%
X.560	110 $\angle 19.88^\circ$	110.79 $\angle 21.04^\circ$	2.15%	4.24 $\angle 12.88^\circ$	4.19 $\angle 13.20^\circ$	1.30%
X.600	110 $\angle 18.50^\circ$	110.91 $\angle 19.61^\circ$	2.11%	4.24 $\angle 11.50^\circ$	4.15 $\angle 11.32^\circ$	2.14%
X.640	115 $\angle 17.13^\circ$	114.36 $\angle 18.52^\circ$	2.48%	0.70 $\angle 10.13^\circ$	0.72 $\angle 10.18^\circ$	2.86%
X.680	115 $\angle 16.91^\circ$	114.92 $\angle 17.44^\circ$	0.93%	0.70 $\angle 36.66^\circ$	0.72 $\angle 36.48^\circ$	2.87%
X.720	115 $\angle 15.53^\circ$	115.64 $\angle 15.64^\circ$	0.59%	0.70 $\angle 35.28^\circ$	0.71 $\angle 35.44^\circ$	1.46%
X.760	115 $\angle 14.16^\circ$	115.19 $\angle 14.20^\circ$	0.18%	0.70 $\angle 33.91^\circ$	0.69 $\angle 33.69^\circ$	1.48%
X.800	115 $\angle 12.78^\circ$	115.19 $\angle 13.12^\circ$	0.62%	0.70 $\angle 32.53^\circ$	0.69 $\angle 32.36^\circ$	1.46%

are 5.32 dB, 11.04 dB, and 3.24%, 5.87%, respectively. The master processor (Intel Galilio Gen version 2, 400 MHz) computes the phasor of a given signal at a reporting rate of 25 phasors per second with the time synchronized to a GPS clock (i.e., SEL 2407). The GPS clock is configured to provide time in Indian Standard Time (IST) format, i.e., [day : hour : minute : second : millisecond].

The developed lab scale PMU prototype based on proposed DDPE algorithm is made available to estimate the phasors of bus-bar voltage and line current at source end during simulated prefault (up to *IST* 286:11:15:36:400), three phase fault (from *IST* 286:11:15:36:400 to *IST* 286:11:15:36:600) and post-fault (from *IST* 286:11:15:36:640 to *IST* 286:11:15:36:960) conditions in experimental radial network.

The above-mentioned hardware results shown in Table IX validate that the developed lab scale PMU can estimate the phasor of voltage and current signals in experimental radial network which are close (i.e., TVE below 3%) to its true/actual phasors obtained using load-flow study. Furthermore, it is also understood that estimated impedance from these phasors by

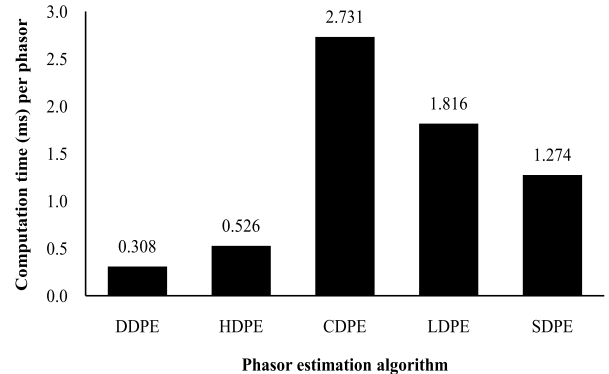


Fig. 20. Time index comparison among phasor estimation algorithms.

the developed lab scale PMU is acceptable according to the IEEE synchrophasor standard. Hence, the developed PMU prototype is also accurate in estimation of phasor of electrical signal in practical power systems and suits in wide area monitoring, control, and protection applications.

Fig. 20 describes the computation time required for estimating the phasor of the voltage and current samples acquired by the sensors for the various methods, i.e., DDPE, HDPE, CDPE, SDPE, and LDPE. The simulation result reveals that proposed method (DDPE) can estimate the phasor of a signal within 0.308 ms whereas other methods like HDPE, CDPE, SDPE, and LDPE spend more time to estimate the phasor as shown in Fig. 20. Furthermore, with the resolution of 0.036° on voltage and current phase angles, accurate voltage and current magnitudes have been achieved by the proposed DDPE. Thus, the proposed algorithm which is also tested on the developed PMU prototype is fast, and can accurately estimate the phasor of a signal in the presence of various electric grid disturbances.

## VI. CONCLUSION

A simple, low cost, and accurate phasor estimation technique suitable for P-class PMU based on the sparse representation of the signals with respect to a suitably chosen dictionary is reported. The performance and robustness of proposed DDPE has been effectively tested and verified as per the test requirements specified in IEEE C37.118.1a-2014 standard and also on modified two-area test power system. The hardware results obtained from an experimental radial power network with developed PMU prototype based on the proposed DDPE have accurately estimated the phasor under transient conditions with an accuracy of TVE less than 3% by utilizing just 10 samples per cycle. The investigation on the performance of proposed estimation technique (DDPE) reveals its significance, i.e., less complexity, high accuracy, and robustness. These advantages of the proposed method make it suitable for estimating phasor corresponding to the fundamental component by a P-class PMU for protection applications. The PMU implementing the proposed DDPE for phasor estimation can be of low cost, and can find applications in monitor and protection of microgrid or distribution network integrated with renewable energy sources.

## REFERENCES

- [1] R. C. Dugan and S. K. Price, "Issues for distributed generation in the US," in *Proc. IEEE Power Eng. Soc. Winter Meeting*, Jun. 2002, pp. 121–126.
- [2] S. M. Brahma and A. A. Girgis, "Development of adaptive protection scheme for distribution systems with high penetration of distributed generation," *IEEE Trans. Power Del.*, vol. 19, no. 1, pp. 56–63, Jan. 2004.
- [3] A. K. Pradhan and G. Joos, "Adaptive distance relay setting for lines connecting wind farms," *IEEE Trans. Energy Convers.*, vol. 22, no. 1, pp. 206–213, Mar. 2007.
- [4] J. A. de la O Serna, "Dynamic phasor estimates for power system oscillations," *IEEE Trans. Instrum. Meas.*, vol. 56, no. 5, pp. 1648–1657, Oct. 2007.
- [5] W. Premerlani, B. Kasztenny, and M. Adamiak, "Development and implementation of a synchrophasor estimator capable of measurements under dynamic conditions," *IEEE Trans. Power Del.*, vol. 23, no. 1, pp. 109–123, Jan. 2008.
- [6] A. G. Phadke and B. Kasztenny, "Synchronized phasor and frequency measurement under transient conditions," *IEEE Trans. Power Del.*, vol. 24, no. 1, pp. 89–95, Jan. 2009.
- [7] R. K. Mai, Z. Y. He, L. Fu, B. Kirby, and Z. Q. Bo, "A dynamic synchrophasor estimation algorithm for online application," *IEEE Trans. Power Del.*, vol. 25, no. 2, pp. 570–578, Apr. 2010.
- [8] M. A. Platas-Garza and J. A. de la O Serna, "Dynamic phasor and frequency estimates through maximally flat differentiators," *IEEE Trans. Instrum. Meas.*, vol. 59, no. 7, pp. 1803–1811, Jul. 2010.
- [9] D. Belega and D. Petri, "Accuracy analysis of the multicycle synchrophasor estimator provided by the interpolated DFT algorithm," *IEEE Trans. Instrum. Meas.*, vol. 62, no. 5, pp. 942–953, May 2013.
- [10] J. A. de la O. Serna, "Synchrophasor estimation using Prony's method," *IEEE Trans. Instrum. Meas.*, vol. 62, no. 8, pp. 2119–2128, Aug. 2013.
- [11] A. T. Muñoz and J. A. de la O Serna, "Shanks' method for dynamic phasor estimation," *IEEE Trans. Instrum. Meas.*, vol. 57, no. 4, pp. 813–819, Apr. 2008.
- [12] D. Belega, D. Macii, and D. Petri, "Fast synchrophasor estimation by means of frequency-domain and time-domain algorithms," *IEEE Trans. Instrum. Meas.*, vol. 63, no. 2, pp. 388–401, Feb. 2014.
- [13] Z. Jiang, S. Miao, and P. Liu, "A modified empirical mode decomposition filtering-based adaptive phasor estimation algorithm for removal of exponentially decaying DC offset," *IEEE Trans. Power Del.*, vol. 29, no. 3, pp. 1326–1334, Jun. 2014.
- [14] E. Ebrahimbzadeh, S. Farhangi, H. Iman-Eini, F. B. Ajaei, and R. Iravani, "Improved phasor estimation method for dynamic voltage restorer applications," *IEEE Trans. Power Del.*, vol. 30, no. 3, pp. 1467–1477, Jun. 2015.
- [15] D. Belega, D. Fontanelli, and D. Petri, "Dynamic phasor and frequency measurements by an improved Taylor weighted least squares algorithm," *IEEE Trans. Instrum. Meas.*, vol. 64, no. 8, pp. 2165–2178, Aug. 2015.
- [16] T. Bi, H. Liu, Q. Feng, C. Qian, and Y. Liu, "Dynamic phasor model-based synchrophasor estimation algorithm for M-class PMU," *IEEE Trans. Power Del.*, vol. 30, no. 3, pp. 1162–1171, Jun. 2015.
- [17] D. Belega, D. Fontanelli, and D. Petri, "Low-complexity least-squares dynamic synchrophasor estimation based on the discrete Fourier transform," *IEEE Trans. Instrum. Meas.*, vol. 64, no. 12, pp. 3284–3296, Dec. 2015.
- [18] A. Zamora *et al.*, "Digital filter for phasor estimation applied to distance relays," *IET Generat., Transmiss. Distrib.*, vol. 9, no. 14, pp. 1954–1963, 2015.
- [19] J. Ren, "Synchrophasor measurement using substation intelligent electronic devices: Algorithms and test methodology," Ph.D. dissertation, Dept. Elect. Eng., Texas A&M Univ., College Station, TX, USA, Dec. 2011.
- [20] S. Affijulla and P. Tripathy, "Development of phasor estimation algorithm for P-class PMU suitable in protection applications," *IEEE Trans. Smart Grid*, vol. 9, no. 2, pp. 1250–1260, Mar. 2018, doi: [10.1109/TSG.2016.2582342](https://doi.org/10.1109/TSG.2016.2582342).
- [21] S. Affijulla and P. Tripathy, "Estimation of phasor under dynamic conditions using convolution," in *Proc. IEEE Power Energy Soc. Gen. Meeting*, Denver, CO, USA, Jul. 2015, pp. 1–5.
- [22] R. K. Mai, L. Fu, Z. Y. Dong, B. Kirby, and Z. Q. Bo, "An adaptive dynamic phasor estimator considering DC offset for PMU applications," *IEEE Trans. Power Del.*, vol. 26, no. 3, pp. 1744–1754, Jul. 2011.
- [23] R. K. Mai, L. Fu, Z. Y. Dong, K. P. Wong, Z. Q. Bo, and H. B. Xu, "Dynamic phasor and frequency estimators considering decaying DC components," *IEEE Trans. Power Syst.*, vol. 27, no. 2, pp. 671–681, May 2012.
- [24] G. Barchi, D. Macii, and D. Petri, "Synchrophasor estimators accuracy: A comparative analysis," *IEEE Trans. Instrum. Meas.*, vol. 62, no. 5, pp. 963–973, May 2013.
- [25] P. Castello, C. Muscas, and P. A. Pegoraro, "Performance comparison of algorithms for synchrophasors measurements under dynamic conditions," in *Proc. IEEE Int. Workshop Appl. Meas. Power Syst. (AMPS)*, Aachen, Germany, Sep. 2011, pp. 25–30.
- [26] J. Ren, M. Kezunovic, and G. Stenbakken, "Dynamic characterization of PMUs using step signals," in *Proc. IEEE Power Energy Soc. Gen. Meeting*, Calgary, AB, Canada, Jul. 2009, pp. 1–6.
- [27] *IEEE Standard for Synchrophasor Measurements for Power Systems*, IEEE Standard C37.118.1-2011, Dec. 2011.
- [28] *IEEE Standard for Synchrophasor Measurements for Power Systems—Amendment 1: Modification of Selected Performance Requirements*, IEEE Standard C37.118.1a-2014, Mar. 2014.
- [29] P. Kundur, *Power System Stability and Control*. New York, NY, USA: McGraw-Hill, 1994.
- [30] A. G. Phadke and J. S. Thorp, *Synchronized Phasor Measurements and Their Applications*. New York, NY, USA: Springer, 2008.

**Shaik Affijulla** (M'14) received the M.Tech. degree in electrical engineering from the National Institute of Technology Hamirpur, Hamirpur, India, in 2011.

He is currently an Assistant Professor with the Department of Electrical Engineering, National Institute of Technology Meghalaya, Shillong, India. His current research interests include the PMU estimation algorithms, application of phasor measurement units for wide-area protection, and power system dynamics.



**Praveen Tripathy** (M'11) received the Ph.D. degree in electrical engineering from IIT Kanpur, Kanpur, India, in 2011.

He is currently an Assistant Professor with the Department of Electronics and Electrical Engineering, IIT Guwahati, North Guwahati, India. His current research interests include wide area monitoring and control, power system dynamics, power system operation and control, facts, power system protection, smart grid, and wind energy systems.

